

Evaluation of Global Ionosphere TEC by Comparison with VLBI Data

Mamoru Sekido¹, Tetsuro Kondo¹, Eiji Kawai¹, Michito Imae²

¹) *Kashima Space Research Center/CRL*

²) *Applied Research and Standards Division/CRL*

Contact author: Mamoru Sekido, e-mail: sekido@crl.go.jp

Abstract

Global Ionosphere map (GIM) produced from world IGS network observation by the CODE was compared with dual frequency geodetic VLBI observation data for evaluation of the accuracy of GIM/CODE. Error spectrum of the GIM/CODE was estimated from the comparison statistically. The GIM/CODE seems to have error of about 3 TECU in low spatial frequency coefficient of the spherical harmonics (SH) expression. About 5 milli-TECU of precision is required to ionosphere TEC map to achieve 1 picosecond precision at observation frequency 8.3 GHz. Estimating from the error spectrum of the GIM/CODE, the GIM will need spherical harmonics up to degrees of about 100 to get such precision. Low correlation was found on TEC rate between GIM/CODE and VLBI data. It should be due to lack of high frequency components in both temporal and spatial scales in the expression of current GIM/CODE. Small (100 km) scale ionospheric disturbances traveling with speed of around 300 km/h are known. The scale of such small structure correspond to SH component in 100 degrees and it can contribute to TEC rate 1 milli-TECU/sec. Thus, 100 degrees of SH expression of ionosphere map every a few tens of minutes might be necessary for practical use of GIM for ionospheric delay and delay rate correction in VLBI observation in the same level with current dual band observations. A pilot project to make precise regional ionospheric map with dense Japanese GPS network (GEONET) is going on. It is interesting to see how accurate TEC map can be produced from dense GPS observations.

1. Introduction

Ionospheric plasma of the earth is a cause of disturbance in space measurement technique using microwave signal such as GPS, VLBI, and spacecraft navigation. Precise ionospheric map is quite useful for those radiometric space measurement systems. Global Positioning System (GPS) technology has been developed dramatically in this decade, and GPS observation sites are distributed all over the world. Now they can be a tool not only for geodesy but also for monitoring the earth environment such as the earth troposphere and ionosphere [1][2]. When a microwave travels in the ionosphere, the signal is delayed by ionospheric plasma in proportional to the total number of free electrons content (TEC) in the ray path. Then dual-frequency GPS receivers are good sensors for ionosphere monitoring [3][4][5][6]. GPS-based TEC measurement has potential to contribute microwave measurement system such as single frequency GPS receiver, VLBI astrometry, and spacecraft navigation. To make clear how much accuracy the global ionospheric map produced from GPS observations has, we compared GPS-based global ionosphere map and VLBI data. Since detailed description on the comparison is in another paper [7], we will review the main part of the comparison and introduce a pilot project to make precise regional ionosphere map over the Japanese Islands from dense GPS network (GEONET).

2. Basic Idea of GPS-Based Ionospheric TEC Evaluation

2.1. Global Ionosphere Model of the CODE

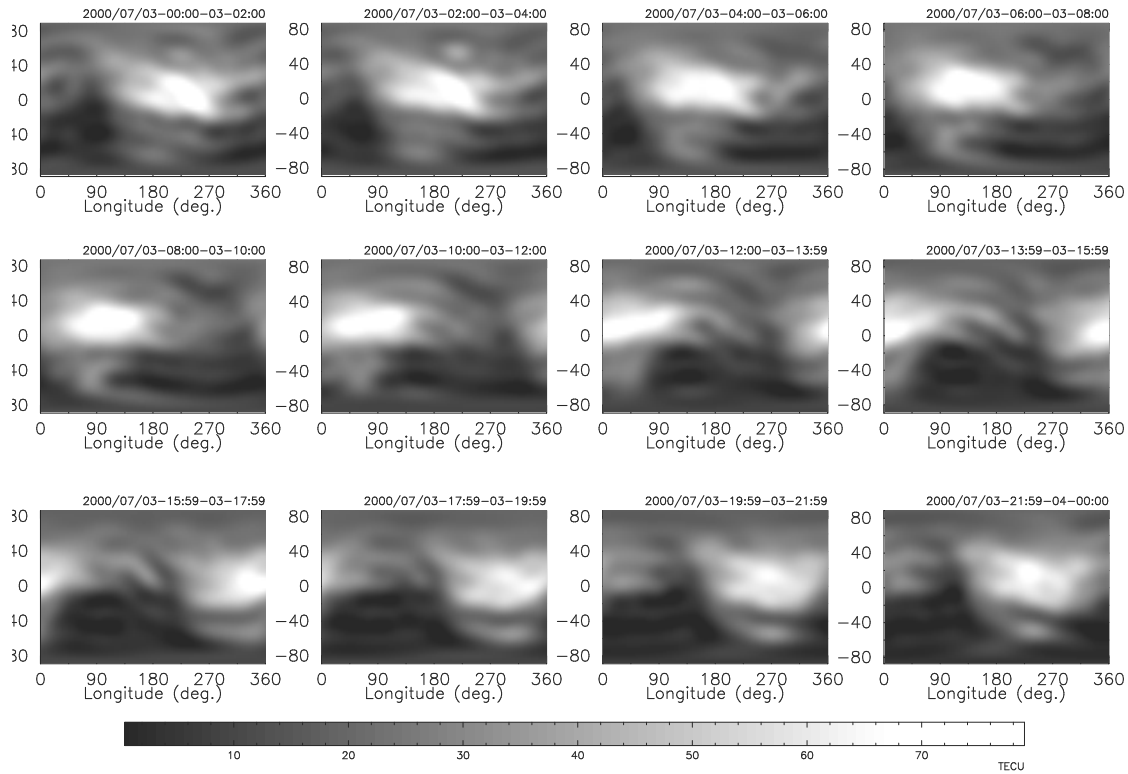


Figure 1. Global ionosphere map on 3rd of July 2000 provided by CODE.

The CODE at Bern University is one of the IGS analysis centers. This institute determines precise GPS orbit by using IGS network observation data and provides the orbit information for world wide GPS users. The CODE has been also routinely generating global ionosphere maps (GIM) on daily basis since 1 January 1996 [9][6] by using more than 130 IGS station's data. Some other IGS analysis centers are generating GIM from GPS data, although we used GIM/CODE for evaluation since it is superior to others at some points. The GIM/CODE is modeled with 256 coefficients of SH expansion up to 15 degrees and 15 orders¹. Thirteen GIMs and their errors in 2 hour intervals (13 maps per day) are included in a GIM/CODE data. The GIM/CODE is regarded as one of the most precise TEC maps generated from GPS observations. The GIM/CODE data is provided in Bernese ION file format and IONOEX format [8], and it is available since 1995 without any interruption. Additionally, the data and related subroutines are accessible through the Internet² any time.

Solar-geomagnetic reference frame or Solar-geographic reference frame is used to express the GIM/CODE. Figure 1 displays an example of TEC map and its error of GIM/CODE data on 5th

¹GIM data in 2000, which was used for this comparison, was expressed with 149 coefficients of 12 degree 8 order of SH.

²<http://www.cx.unibe.ch/aiub/ionosphere/>

Table 1. VLBI Experiments used for TEC comparison

Date	Experiment name	Station name
2000/4/7-18	6 KSP sessions	Kashima11, Koganei
2000/7/5-6	NEOS-A375	Algonquin, Fortleza, Kokee, Wettzell, Gilcreek
2000/7/10-11	CORE-1001	Algonquin, Gilcreek, Hartrao, Hobart, Matera, Tsukuba
2000/7/11-12	NEOS-A376	Algonquin, Fortleza, Kokee, Nyales, Wettzell,
2000/7/12-13	CORE-3001	Gilcreek, Kokee, Onsala, Westford, Wettzell
2000/7/18-19	NEOS-A377	Algonquin, Fortleza, Kokee, Wettzell, Gilcreek,
2000/7/25-26	NEOS-A378	Algonquin, Fortleza, Kokee, Nyales, Wettzell

July 2000. It is expressed in geographical coordinates, hence it is seen that the TEC structure is meandering along geomagnetic equator.

2.2. Comparison of VLBI-Based TEC and GIM

The GPS technique can measure the TEC along the ray path from GPS satellite to an observation station, whereas VLBI measure the difference of TEC in the ray path to the radio source between two stations. Then TEC measured by VLBI and that by GPS were compared with the following procedures. (i) The coordinates of ionospheric point, which is the intersection between ionospheric layer and line of sight from VLBI station to the observed radio source at VLBI observation epoch, is calculated. Then vertical TEC value at that location is computed from GIM/CODE maps. (ii) Slant TEC is computed from the vertical TEC by taking into account a ionosphere mapping function, then difference of the slant TECs between two stations is taken as $VTEC_y \cdot Fm(El_y) - VTEC_x \cdot Fm(El_x)$, where $VTEC_i$ is ionospheric TEC in zenith direction. GIM/CODE has been using isotropic spherical single layer mapping function as

$$Fm(El) = \frac{1}{\cos\{\sin^{-1}[\frac{R}{R+H} \cos(El)]\}}, \quad (1)$$

where R is earth radius, and ionosphere height from earth surface is assumed to be constant $H=450$ km. (iv) Finally the derived GPS-based TEC is compared with VLBI-based TEC.

Precision of VLBI-based TEC measurement is simply determined by group delay measurement precision and its error is evaluated by signal to noise ratio (SNR). By supposing that error of VLBI-based TEC measurements is known, then error of GPS-based TEC map can be evaluated statistically. Even the comparison of TEC map with VLBI data is relative difference of slant TEC at two points of earth ionosphere, that has sensitivity to vertical absolute TEC through mapping function. Thus as far as the error of the TEC map follows appropriate mapping function, the error in slant TEC can be projected upon the vertical absolute TEC value. This is basic idea of evaluating TEC map accuracy by comparison with VLBI data.

Each quantities for comparison from GPS and VLBI are modeled as follows:

$$dTEC_{GIM} = (VTEC_y + \epsilon_{GIM,y}) \cdot Fm(El_y) - (VTEC_x + \epsilon_{GIM,x}) \cdot Fm(El_x) \quad (2)$$

$$dTEC_{VLBI} = STEC_y - STEC_x + \epsilon_{VLBI}, \quad (3)$$

and supposing $\langle \epsilon_{VLBI}^2 \rangle$ is known from VLBI data, ϵ_{GIM} is evaluated statistically.

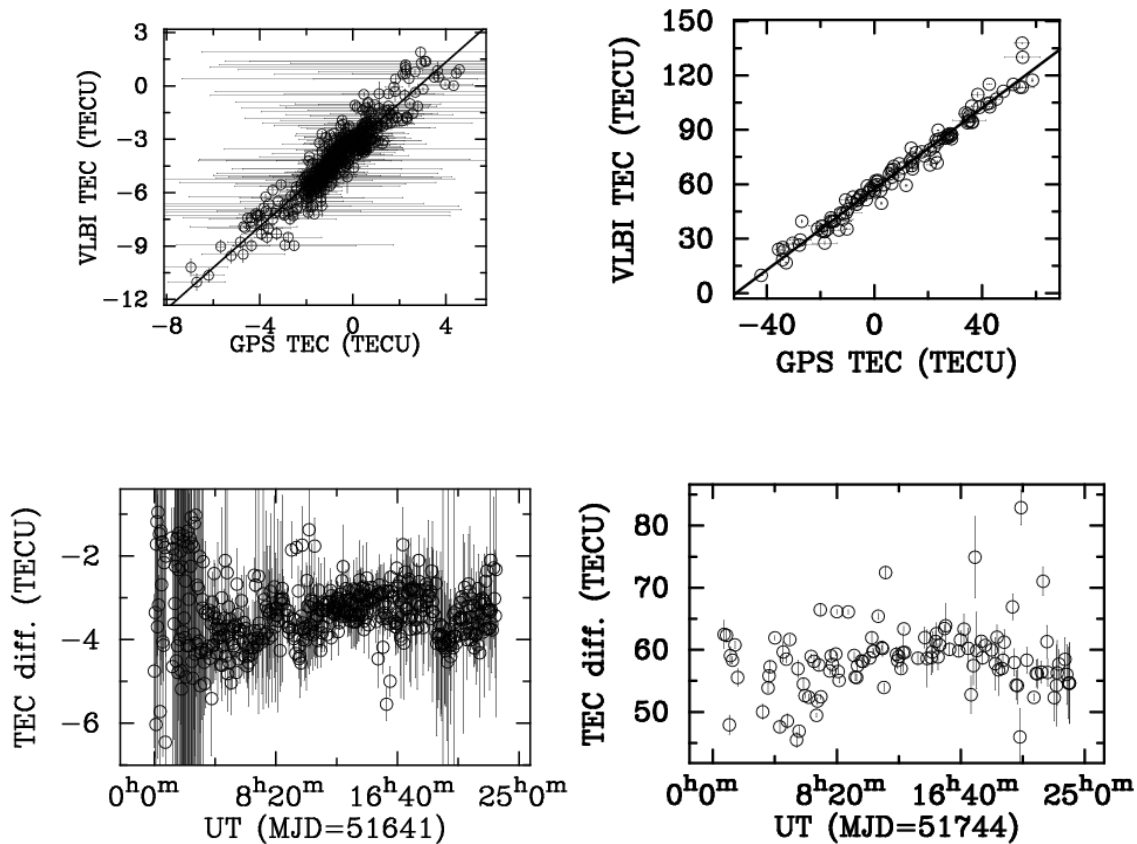


Figure 2. Correlation (upper panels) and difference (lower panels) between GIM/CODE and VLBI data. (Left): Kashima-Koganei (109km) baseline on 7 April 2000. The correlation coefficient, proportional coefficient, and offset were respectively 0.93, 1.01, and -3.4 TECU. Root-mean-square (RMS) difference was 0.77 TECU. (Right): Algonquin-Wettzell (6000km) baseline on 18 June 2000. The correlation coefficient, proportional coefficient, and offset were respectively 0.99, 1.13, and 57.6 TECU. The RMS of the difference was 5.4 TECU. The offsets comes from S/X VLBI receiver offset (see section 5).

3. Comparison of TEC

3.1. Statistical Comparison between VLBI and GPS-Based TEC Map

Six KSP (Kashima11-Koganei) VLBI experiments (2683 scans) and six intercontinental VLBI experiments (total 6855 scans of 37 baselines) are used for the comparison (Table 1). Correlation and difference between VLBI-based TEC and that computed from GIM/CODE are plotted in Figure 2 as an example.

To evaluate GIM error correctly we need to remove the factor of mapping function and to survey the characteristic of baseline dependency. For this purpose, we divided the whole data set into several subsets by elevation angles and baseline lengths. Then mean square of TEC difference between VLBI and GIM are computed for each subset. Mathematical expression of this procedure might be derived from equation (2), (3) as follows (see appendix A of [7]):

$$\langle \Delta TEC^2 \rangle \cong \sigma_{\text{GIM}}^2 \langle Fm^2(El_x) + Fm^2(El_y) \rangle + \sigma_{\text{VLBI}}^2, \quad (4)$$

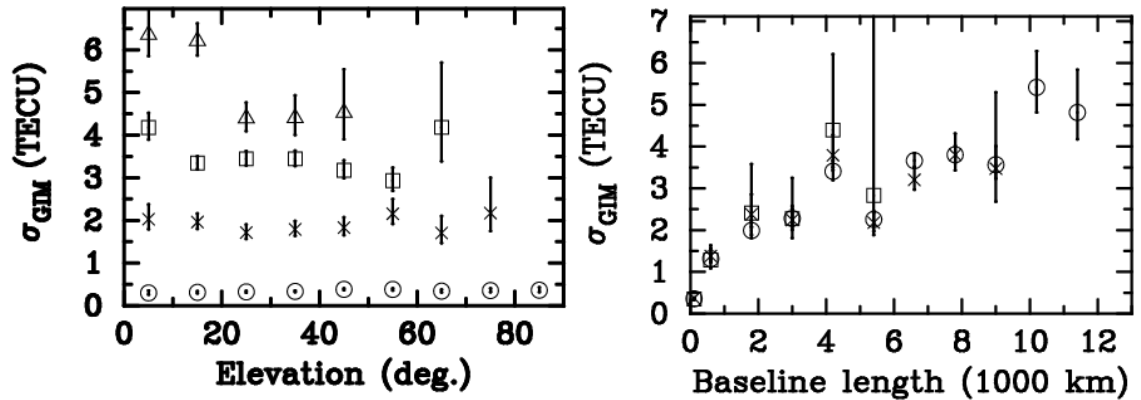


Figure 3. Estimated GIM/Code TEC error is plotted with respect to elevation angle (left panel). TEC difference (GPS - VLBI) data set was divided into data subset by 10 degree intervals of lower elevation angle of the VLBI station pair. The data subsets were again divided into 4 groups by the baseline length, \circ : 0 – 500 km (KSP), \times : 500 – 4000 km, open box: 400 – 8000 km, and \triangle : longer than 8000 km. The GIM/Code error was computed by using equation (5). Estimated GIM/Code errors are plotted with respect to baseline length in right panel. The data was divided into subsets by 1200 km interval of baseline length except for the KSP data (109 km). Elevation cut-off test was also performed at elevation limit 20 (\circ), 40 (\times), and 60 (open box) degrees. The error bars in the plots indicate 95% confidence interval.

where $\Delta TEC = dTEC_{GIM} - dTEC_{VLBI}$. Since σ_{VLBI}^2 is supposed to be known, error of GIM is evaluated by

$$\sigma_{GIM} = \sqrt{\frac{\langle (\Delta TEC)^2 \rangle - \langle \sigma_{VLBI}^2 \rangle}{\langle Fm^2(El_x) + Fm^2(El_y) \rangle}}. \quad (5)$$

for each data subset and plotted in Figure 3. The flat elevation dependency of the left panel indicates the mapping function and the statistical treatment are appropriate. The baseline dependency is plotted with data sets of elevation cutoff test (20, 40, and 60 degrees). Since plots of elevation cutoff test almost coincide regardless different elevation cutoff angles, it indicates that factor of mapping function is appropriately calibrated and GIM error is projected to vertical one correctly. Interpreting the baseline dependency of σ_{GIM}^2 as structure function of GIM error $R(l) = \langle (er(x) - er(x+l))^2 \rangle$, power spectrum of GIM error can be computed from it. Figure 4 (left) shows the σ_{GIM} dependency on geocentric angle. Since structure function is monotonically increasing function, two sorts of lines are drawn as test models of the structure function. Auto-correlation function of GIM error computed from the test models are superimposed in right lower corner of the figure. Two error spectrum models of GIM, which is estimated from the structure function, are displayed in the right panel. Mean-square of SH coefficients and errors of each coefficient attached with the GIM/Code data are also plotted in the same figure. Two conclusions on precision of GIM/Code are inferred from this figure. The GIM/Code seems to have error around 3 TECU in lower spectrum of SH expression. Ionospheric delay of 1 picosecond corresponds to 0.05 TECU at radio frequency 8.3 GHz. Therefore to use GIM/Code for ionospheric delay correction in the same precision with current geodetic VLBI, about one hundred of order of SH expansion will be necessary.

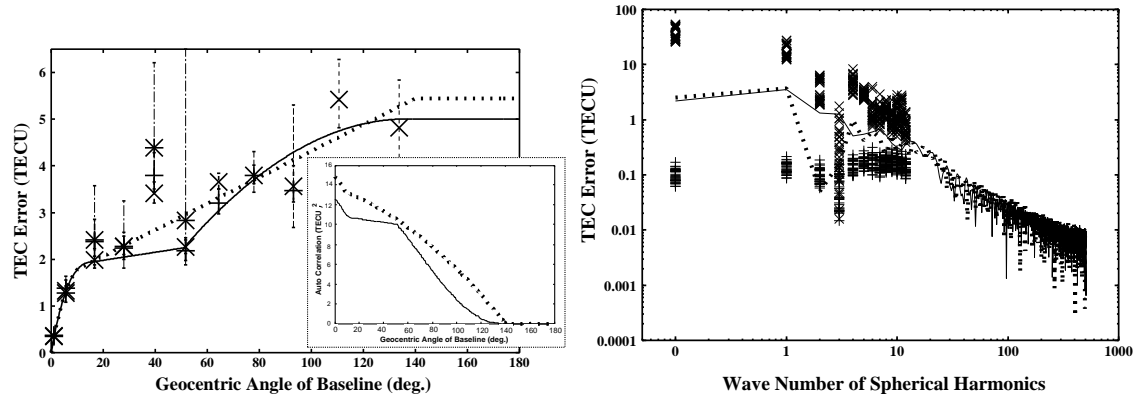


Figure 4. (Left): Square-root of structure function of TEC error. Three kinds of marks correspond to data of elevation cut-off test (20, 40, and 60 degrees). Solid and broken lines are two kinds of models of structure function composed of three truncated functions. Small screen at right corner shows auto-correlation functions derived from two models of structure functions. (Right): TEC error spectrum of GIM/CODE model. Solid line and broken line correspond to the structure function models in left panel. Mark “x” indicates root-sum-square of SH components of GIM/CODE, and “+” indicates root-sum-square of errors attached with GIM/CODE data. Larger index between degree and order of SH index set was used as wave number and the root-sum-square was taken for the same wave number. Horizontal coordinate 0 is indicated at coordinate of 0.1 to express DC component of the error spectrum.

4. Comparison of TEC Rate

TEC rates between VLBI measurements and counterpart computed from GIM/CODE data also were compared. VLBI-based TEC rate consists of the temporal variation of TEC and spatial change of the line of sight due to tracking of radio source. We computed TECs in line of sight to radio source at desired epoch and at other 4 epochs with 10 minute intervals before and after the desired epoch. Then TEC rate was derived by numerical derivation by using the 5 points of TEC data.

The TEC rates comparison was performed from short baseline (KSP) to intercontinental baseline (IVS data listed in Table 1). Unfortunately correlation between VLBI-based TEC rate and TEC rate computed from GIM/CODE was almost close to zero for short (109 km) baselines. Some correlation around 0.6 – 0.8 were found on longer baselines, although it was far from the accuracy for phase delay rate correction. Figure 5 shows an example of TEC rate comparison result of Algonquin - Wettzell baseline on 18th July 2000. RMS difference of TEC rate between the GIM/CODE and VLBI is several milli-TECU per second, which is one order larger than the accuracy of TEC rate needed for delay rate correction in VLBI observation at radio frequency 8.3 GHz. The reason for the poor coincidence of TEC rate is understood by following two reasons. (i) The GIM/CODE data has time resolution of 2 hours. Thus shorter time scale TEC variation is not included in the data. (ii) The GIM/CODE data compared here are expressed with up to 12 degrees 8 orders of SH components. Then ionospheric TEC structure smaller than a minimum spatial scale (2500 km x 1700 km) is not contained in the data. The lack of higher frequency component in both time and spatial domain in GIM/CODE will be the main cause of low precision of TEC rate derived from GIM/CODE.

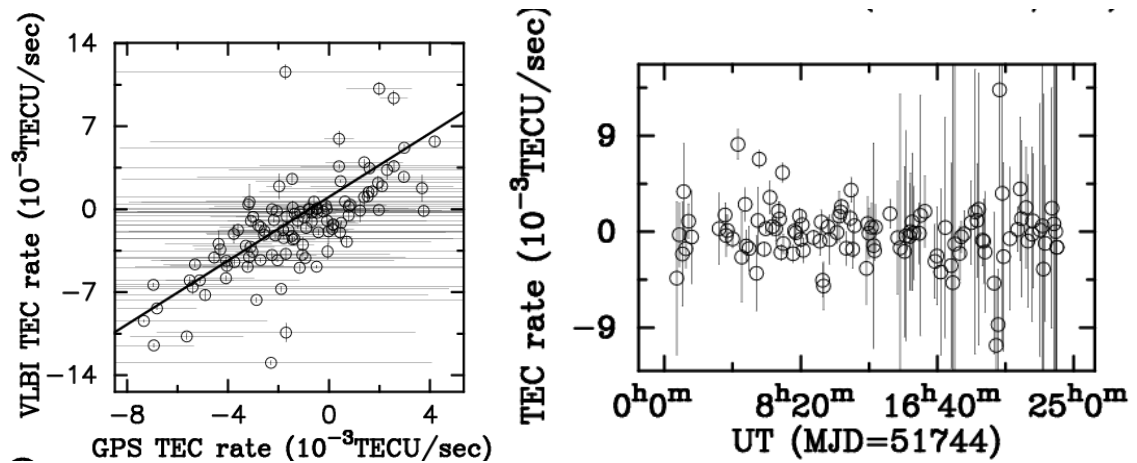


Figure 5. Comparison of TEC rate between GIM/CODE and VLBI data on 18 July 2000 on Algonquin - Wettzell baseline. The TEC rate of GIM/CODE were computed by numerical derivation. Left panel shows scatter plot of TEC rate measured by VLBI and counterpart computed from GIM/CODE. Right panel is residual plot of the TEC rate difference between GIM/CODE model and VLBI data. Correlation was 0.7 and the RMS residual was 2.9×10^{-3} .

5. S/X VLBI Receiver Offset

From comparison between GPS-based TEC measurements and VLBI data, difference of signal transmission delay between X-band and S-band of VLBI receiver system is derived as a by-product. Since most of the offsets (difference of 0 point between VLBI and GPS in Figure 2) derived from these comparisons were almost constants for each baseline regardless of difference of experiments, it is sure that these offsets originate from each VLBI station. This S/X VLBI receiver offset does not come only from hardware but also it can be introduced by manual operation of phase calibration (PCAL) data. Actually, the offsets on Kokee station related baselines in CORE-3001 were inconsistent with ones of other experiments. It is known that manual pcal phase was used for Kokee station, and that operation of PCAL data on Kokee related baseline might cause the shift of the offset in CORE-3001 experiment. Table 2 shows the S/X VLBI receiver offset at each station computed by least square method under the constraint that total sum of the offset equals to zero. The constraint was used because we have no a priori knowledge of absolute value of the offset at any station. Then relative values in the table have meaning but the absolute values may not.

This (hardware) delay offset between S and X band VLBI receivers has not been made aware in normal geodetic VLBI observation, because it is normally absorbed in station clock offset in the analysis. These have already been pointed out by T. Herring [10]. But these offsets were not actually measured due to lack of independent measurements of ionospheric TEC to distinguish the VLBI receiver offsets from the ionospheric dispersive delay. Attention may have to be paid to these offsets when precise calibration of station delay is needed such as VLBI experiment for precise time transfer or VLBI observation with phase delay.

Station	offset (n sec)	Error (n sec)
Algonquin	-0.43	0.4
Fortleza	-5.3	0.4
Gilcreek	0.13	0.4
Hobart	1.2	0.6
Hartrao	-16.5	0.6
Kokee	-18.4	0.4
Wettzell	13.6	0.4
Westford	0.5	1
Tsukuba	5.6	0.6
Nyales	-0.4	0.6
Onsala	14.4	0.8
Matera	5.5	0.5

Table 2. VLBI receiver offset derived from comparison between VLBI-based TEC and GPS-based TEC. Each station's offsets were derived with assuming that sum of all stations offsets equals to 0. Error is formal error of least square solution. To make reduced- χ^2 equal to unity, square of extra 1.2 nanoseconds of error was added to square of each error.

6. Small Scale Structure of Ionosphere

Geographical Survey Institute (GSI) of Japan is operating about 1000 GPS receivers placed on the Japanese Islands. That system is named GEONET [11], since it is thought to be not only a sensor for crustal deformation but also a sensor for earth environment including atmosphere and ionosphere. Saito et al. [12] demonstrated the presence of small scale traveling ionosphere turbulence (TID), which has 100 km scale with about 1 TECU amplitude (Figure 6). One hundred km scale on the earth surface correspond to SH component at 100 degrees, and it corresponds to the conclusion derived from comparison with VLBI data in Section 3.1. The traveling speed of the TID is around 300 km/hour, thus TID with 1 TECU of amplitude can cause 1 milli-TECU/sec, which is in the same order with the residual of TEC rate comparison (Figure 5) in Section 4. Thus this sort of TID needs to be included in ionosphere TEC map model from both delay and delay rate viewpoints. Ping et al. [13] has made a regional ionosphere map (RIM) expressed by 60 degrees and orders of SH expansion every 10 minutes interval from joint use of GEONET data and GIM/CODE. Currently we are collaborating for accuracy evaluation of the RIM.

7. Conclusions

Accuracy of GIM/CODE was evaluated by comparison with VLBI data on various baselines. Error spectrum of the GIM/CODE was derived from the statistical comparison. The GIM/CODE seems to have about 3 TECU of error at low degree of SH components. To apply ionospheric delay correction to VLBI data (X-band) with the GIM/CODE at accuracy of 1 picosecond, accuracy of 50 milli-TECU is necessary. Estimating from the obtained error spectrum of GIM/CODE, about 100 degree of SH expansion will be necessary to achieve that accuracy. TEC rate was compared with VLBI data, too. However, the difference was one order larger than required accuracy. The poor coincidence should be caused from lack of high frequency components in the data in both temporal and spatial scale.

Presence of small (100 km) scale ionospheric disturbances with 1 TECU magnitude are known and they travel about 300 km per hour. This order of spatial scale also corresponds to SH component at about 100 degrees. This sort of TID needs to be included in ionospheric TEC model for practical use in VLBI ionospheric delay and delay rate correction. Ping et al. [13] has made high

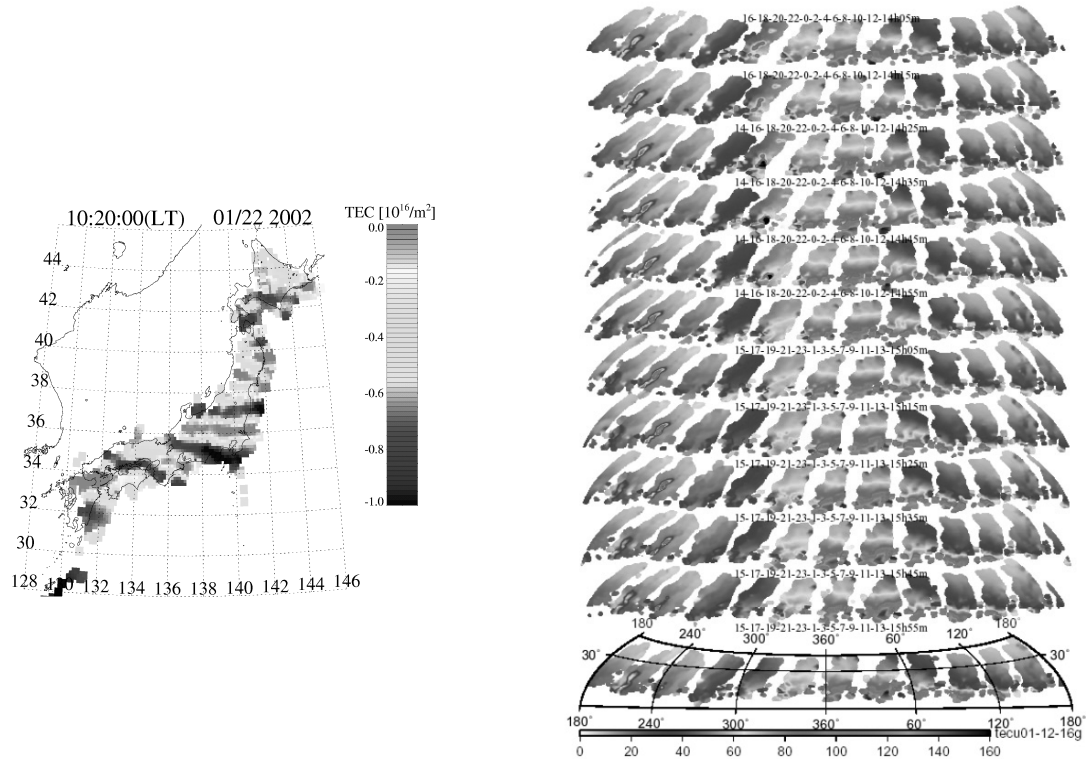


Figure 6. Traveling ionospheric disturbance (TID) detected with GEONET by Saito et al.[12] (left) and Regional Ionosphere map (RIM) made from joint use of GIM/CODE and GEONET data by Ping et al.[13](right). The RIM is expressed by 60 degree of SH expansion at every 10 minutes interval.

resolution regional ionospheric model over the Japanese Islands from joint use of GEONET data and GIM/CODE. The RIM is expressed with SH expansion of 60 degrees and orders, and its time interval is 10 minutes. Evaluation and improvement of the RIM by comparison with VLBI and with satellite data (Topex/Poseidon) is going on. This project is interesting to see how accurate an ionospheric map can be derived from dense GPS network.

As a by-product of the comparison between VLBI and GPS-based GIM, S/X VLBI receiver biases are detected. This bias was pointed out by T. Herring [10], however it was not obvious because it is easily absorbed in clock parameters in VLBI analysis.

This comparison was made with data in 2000, when the GIM/CODE was expressed with 12 degrees and 8 order of SH expansion. Now the model of GIM/CODE is updated to 15 degrees and 15 order of SH expansion. Thus the precision of the map might be somewhat improved than these results, although basic sense of the conclusion in this paper may not be changed.

Acknowledgments Authors thanks Stefan Schaer at Bern University for providing GIM data and related subroutines. This research has made use of international geodetic VLBI data provided by the International VLBI Service for Geodesy and Astrometry.

References

- [1] Beutler, G., EXECUTIVE SUMMARY, *IGS Analysis Center Workshop*, 9-18,1998.
- [2] Feltens J., and S. Schaer, IGS PRODUCTS FOR THE IONOSPHERE, *IGS Analysis Center Workshop*, 225-232,1998.
- [3] Lanyi G. E., and T. Roth, A comparison of mapped and measured total ionospheric electron content using global positioning system and beacon satellite observations, *Radio Sci.*, *23*, 483-492. 1988.
- [4] Wilson B. D., J. A. Mannucci, and D. C. Edwards, Subdaily northern hemisphere ionospheric maps using an extensive network of GPS receivers, *Radio Sci.*, *30*, 639-648, 1995.
- [5] Ho C. M., Wilson B. D., J. A. Mannucci, J. U. Lindqwister, N. D. Yuan, A comparative study of ionospheric total electron content measurements using global ionospheric map of GPS, TOPEX radar, and the Bent model, *Radio Sci.*, *32*, 1499-1512, 1997.
- [6] Schaer S., Mapping and Predicting the Earth's Ionosphere Using the Global Positioning System, *Ph.D. thesis at Bern University*, 1999.
- [7] Sekido M., T. Kondo, E. Kawai, & M. Imae, Evaluation of GPS-based ionospheric TEC map by comparing with VLBI data, *Radio Science*, *38*, 1069-1090, 2003.
- [8] Schaer S., W. Gurtner, and J. Feltens, IONEX: The ionosphere Map EXchange Format Version 1, *Proc. of IGS Analysis Center Workshop, ESA/ESOC Darmstadt in Germany, February 9-11 1998*, 233-247, 1998.
- [9] Schaer S., G. Beutler, and M. Rothacher, MAPPING AND PREDICTING THE IONOSPHERE, *Proc. IGS Analysis Center Workshop 1998, ESA/ESOC Darmstadt in Germany, February 9-11 1998*, 307-318, 1998.
- [10] Herring T. A., The precision and accuracy of intercontinental distance determinations using radio interferometry, *Ph.D. thesis at the Massachusetts Institute of Technology*, section 4.1.1, 1983.
- [11] Miyazaki S., T. Saito, M. Sasaki, Y. Hatanaka, and Y. Iimura, Expansion of GSI's Nationwide GPS Array, *Bull. Geogr. Surv. Inst.*, *43*. 23-34, 1997.
- [12] Saito A., S. Fukao, and S. Miyazaki, High resolution mapping of TEC perturbations with the GSI GPS network over Japan, *Geophys. Res. Lett.*, *25*, 3079-3082, 1998.
- [13] Ping J., Y. Kono, K. Matsumoto, Y. Otsuka, A. Saito, C. Shum, K. Heki, and N. Kawano, *Earth Planets Space*, *54*, e13-e16, 2002.